Photosynthetic Water Oxidation at High O_2 Backpressure Monitored by Delayed Chlorophyll Fluorescence†

Jürgen Clausen,‡ Wolfgang Junge,‡ Holger Dau,*,§ and Michael Haumann*,§

Universität Osnabrück, FB Biologie/Chemie, Abt. Biophysik, Barbarastrasse 11, D-49069 Osnabrück, Germany, and Freie Universität Berlin, FB Physik, Arnimallee 14, D-14195 Berlin, Germany

Received June 21, 2005; Revised Manuscript Received July 26, 2005

ABSTRACT: The atmospheric dioxygen is produced by photosynthetic organisms. This light-driven process culminates in what appears as one step: a four-electron abstraction from two water molecules bound to the Mn_4Ca complex of photosystem II. Recently, an intermediate of the O_2-producing reaction sequence was stabilized by elevated oxygen backpressure and detected by UV flash photometry [Clausen, J., and Junge, W. (2004) *Nature 430*, 480]. We scrutinized its properties by delayed chlorophyll fluorescence measurements. Half-suppression of oxygen evolution was observed at a similar O_2 pressure of 2.3 bar, as previously, now with photosystem II membrane particles from spinach, without artificial electron acceptors, and at a high signal-to-noise ratio. The data are tentatively interpreted as the stabilization of a 2-fold oxidized state of the catalytic center (S_2*) with bound peroxide and its slow conversion into the normal S_2 state by the release of peroxide.

Plants, algae, and cyanobacteria oxidize water and produce dioxygen in photosystem II (PSII).[1] The catalytic center comprises a Mn_4Ca complex bound to the D1 subunit of PSII, the atomic structure of which is now emerging from crystallographic (*1*, *2*) and X-ray absorption spectroscopy studies [(*3*, *4*) and references therein]. The growing structural information calls for in-depth investigations on the crucial reaction sequence of oxygen evolution to unravel its still enigmatic chemical mechanism.

Clocked forward by the absorption of four quanta of light, the catalytic center acquires increasingly higher oxidation states (*5*) (starting from S_0 to reach S_1 (dark stable), S_2, S_3, and $S_3Y_Z^{ox}$, wherein Y_Z denotes a special, redox-active tyrosine). The terminal dark reaction ($S_3Y_Z^{ox} \rightarrow S_0$) closes the cycle and is coupled to the release of dioxygen. One view is that, upon reaching the highest oxidation state, four electrons are abstracted from two molecules of bound water to liberate dioxygen so that $S_3Y_Z^{ox}$ is reduced to S_0. Until recently, the latter reaction appeared as a single step without a detectable intermediate. Evidence for the existence of such an intermediate has been provided in a study employing elevated oxygen pressure (*6*). An O_2 pressure of only 2.3 bar (about 10-fold higher than ambient) half-inhibited the liberation of oxygen by stabilizing an intermediate. This intermediate was tentatively ascribed to a 2-fold-oxidized manganese complex (similar to state S_2), which possibly carries a bound peroxide.

In this investigation, we used recombination chlorophyll fluorescence after laser-pulse excitation (the so-called delayed fluorescence, DF) to monitor the redox state of the catalytic center at elevated oxygen pressure. DF stems from the reversal, in a thermally activated process, of the flash-light-induced charge separation in PSII (*7*). Its intensity reflects the free energy of the reached charge-separated state with respect to the excited antenna state (*7*). The various kinetic phases of DF transients reflect the partial reactions of the electron-transfer chain $Mn \rightarrow Y_Z \rightarrow P_{680}^+$, wherein Mn denotes the catalytic metal complex and its ligands, Y_Z denotes the Tyr-161 on the D1 subunit, and P_{680}^+ denotes the photooxidized chl*a* moiety that drives these reactions (for a comprehensive description of the DF method as applied to PSII see ref *7*). The major advantage of DF over UV (see ref *6*) and X-ray flash spectroscopy (see ref *4*) is its very high signal-to-noise ratio. It allows single-shot experiments at microsecond time resolution even with scattering samples, like PSII membrane particles from spinach, as used in this study.

By the DF technique, we corroborated the previously found stabilization of an intermediate by elevated oxygen pressure (*6*) but now with PSII of a higher plant in its native membrane and without the complication of added electron acceptors. A plausible assumption is that this intermediate is equivalent to $(H_2O_2)S_2$*Y_Z. Presumably, this state slowly decays, within less than 700 ms, perhaps to yield the normal 2-fold oxidized S_2 state of the catalytic center by releasing the bound peroxide. This finding together with kinetic evidence for another intermediate, as detected by time-

† Financial support provided by the Deutsche Forschungsgemeinschaft (Grants C6 and C8 within SFB 498 to H.D. and M.H. and Grant Ju97/15-1,2 to W.J.), the Fonds der Chemischen Industrie, and the Land Niedersachsen (to W.J.) is gratefully acknowledged.

* To whom correspondence should be addressed: FB Physik, Freie Universität Berlin, Arnimallee 14, D-14195 Berlin, Germany. Telephone: +49-30-8385-6101. Fax: +49-30-8385-6299. E-mail: haumann@physik.fu-berlin.de (M.H.); FB Physik, Freie Universität Berlin, Arnimallee 14, D-14195 Berlin, Germany. Telephone: +49-30-8385-3581. Fax: +49-30-8385-6299. E-mail: holger.dau@physik.fu-berlin.de (H.D.).

‡ Universität Osnabrück.

§ Freie Universität Berlin.

[1] Abbreviations: chl, chlorophyll; DF, delayed-fluorescence emitted by the chlorophylls of PSII; P_{680}, primary electron donor of PSII; PSII, photosystem II, S_i, oxidation states in the S-state cycle of water oxidation; Y_Z, tyrosine-161 of the D1 protein of PSII.

10.1021/bi051183a CCC: $30.25 © 2005 American Chemical Society
Published on Web 08/25/2005

resolved X-ray absorption spectroscopy (*8*), might offer a clue to unravel the whole reaction sequence of oxygen evolution.

MATERIALS AND METHODS

PSII-enriched membrane particles were prepared from market spinach with 1 M glycine betaine present as a stabilizer in all media (*9*) and frozen at −80 °C until use. Their O_2-evolution activity determined by a Clark electrode was ∼1200 μmol of O_2 (mg of chl)$^{-1}$ h^{-1}. For DF measurements, PSII membranes were thawed and diluted at 20 μg of chl mL^{-1} in buffer B (1 M glycine betaine, 10 mM NaCl, 5 mM $CaCl_2$, and 25 mM MES at pH 6.5). The presence of about 5 plastoquinone molecules per PSII allowed ∼10 turnovers/PSII reaction center. Thus, the addition of an artificial electron acceptor was not necessary.

Kinetic delayed chlorophyll fluorescence measurements (DF) were performed at room temperature (∼20 °C) with the setup described in ref *7* using a gated photomultiplier for monitoring DF transients. The same optical cell with fused quartz windows sustaining pressures up to 30 bar as described in ref *6* was used for the DF experiments. Dark-adapted PSII samples were excited by trains of saturating flashes from a Continuum Minilite-II laser (frequency-doubled, Q-switched Nd:YAG, $\lambda = 532$ nm, full width at half-maximum of ∼5 ns, flash spacing of 700 ms, attenuated to 2 mJ cm^{-2}). The laser beam was shaped by appropriate optics to homogeneously illuminate the whole sample volume. DF transients were corrected for a small DF contribution of the quartz windows as outlined in ref *7*. Transients were recorded on a personal computer equipped with a 20 MHz A/D card (Adlink) and in-house software using an averaging algorithm resulting in logarithmic spacing of data points starting at 20 μs after the laser flash (electrical bandwidth set by a Tektronix amplifier to 1 MHz).

PSII samples were equilibrated with elevated oxygen (or He) pressure as follows: (1) 100 mL of buffer B was pre-equilibrated at the desired $p(O_2)$ for 30 min in a stainless-steel pressure cell under stirring. (2) 3 mL of the pre-equilibrated buffer was filled in the cuvette (optical path length of 1 cm) containing a magnetic stirring bar; the cuvette then was mounted into the optical cell. (3) The cell was pressurized and further equilibrated for 10 min under stirring. (4) An aliquot of the PSII membranes (∼50 μL) was injected by a syringe into the pressurized cell, and the solution was stirred in the cuvette for 20 min in darkness before application of the laser flashes. O_2 gas was of the highest available purity.

RESULTS

Figure 1 shows DF transients for up to 10 ms after the 1st, 2nd, and 3rd Laser flash, which was applied to dark-adapted PSII membrane particles at ambient (i.e., 0.21 bar) (A) and 20 bar (B) partial pressure of oxygen. The initial extent of DF (at 20 μs) after flashes 1 and 2 was unchanged by elevated oxygen pressure, and most of the decay occurred rapidly, within microseconds (Table 1). We conclude that the electron-transfer $Mn_4 \rightarrow Y_Z \rightarrow P_{680}^+$ during the $S_1 \rightarrow S_2$ and $S_2 \rightarrow S_3$ transitions is not strongly affected by elevated $p(O_2)$.

The DF transient on the 3rd flash depends strongly on $p(O_2)$. At ambient $p(O_2)$ of 0.2 bar, the rapid initial decay

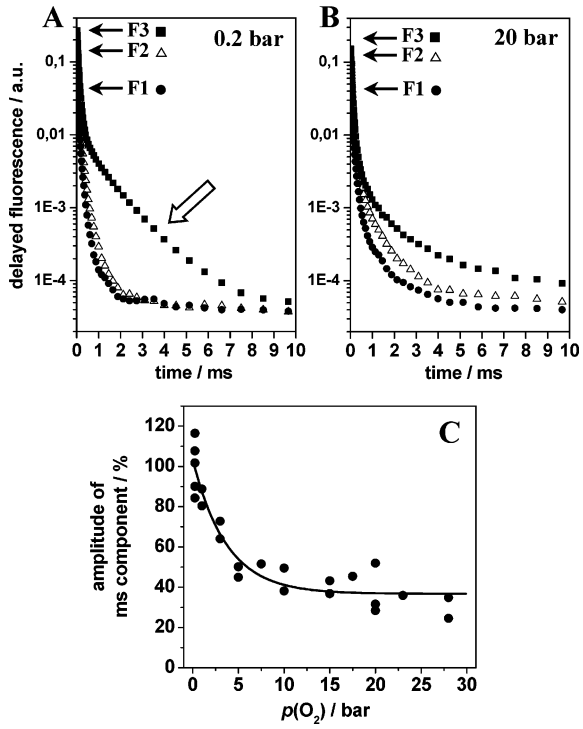

FIGURE 1: Delayed fluorescence transients recorded with PSII membranes on laser flashes 1, 2, and 3 at ambient $p(O_2)$ of (A) 0.2 bar and (B) 20 bar. The arrow in A emphasizes the DF decay with $\tau \approx 1.2$ ms attributable to the O_2-evolving transition on flash 3. Each transient represents the average of three measurements. Note the logarithmic scale of the *y* axis. (C) Normalized intensities integrated from 0.5 to 5 ms of the DF transients on flash 3 as a function of $p(O_2)$. The line represents a single-exponential simulation with a $p(O_2)_{1/2}$ of 2.3 bar.

Table 1: Amplitudes (I_i) and Relaxation Times (τ_i) of a Triexponential Fit of the Decay of the DF Transients Shown in Figure 1[a]

flash number	$p(O_2)$/bar	I_1	τ_1	I_2	τ_2	I_3	τ_3
1	0.2	19.27	0.071	1.47	0.25	0.03	4.3
	20	19.63	0.072	0.81	0.39	0.04	4.4
2	0.2	62.03	0.053	4.21	0.25	0.03	4.1
	20	53.11	0.064	1.68	0.53	0.05	4.6
3	0.2	95.93	0.074	3.95	1.17	0.12	4.5
	20	69.39	0.067	2.01	0.59	0.37	4.7

[a] The amplitudes are given in percent of the total summed amplitudes for the 3rd flash transient at 0.2 bar O_2; relaxation times are given in milliseconds. Oxygen pressure and flash number are as indicated.

of the DF occurred with a relaxation time of ∼70 μs and was completed after less than 500 μs. This DF decay in part reflects the slowest component of the electron transfer from Y_Z to P_{680}^+, which presumably is rate-limited by relaxation processes at the level of Y_Z (*10*). It was followed by a prominent slower decay phase (Figure 1A, arrow) with a relaxation time τ_2 of ∼1.2 ms (Table 1). Because this phase was observed on the 3rd flash and its magnitude oscillated with a period of four (see below), it is attributed, as previously indicated (*7*), to the reduction of $S_3Y_Z^{ox}$ during the O_2-evolving reaction.

At 20 bar O_2, on the 3rd flash, the decay of the largest DF portion ($\tau \approx 70$ μs) was similar to that at 0.2 bar (Table 1). The fact that the rapid decay was not affected by elevated oxygen pressure is in line with the previously reported reduction of P_{680}^+ in nanoseconds at 20 bar oxygen pressure as recorded by absorption transients at 827 nm (*11*, *12*). High

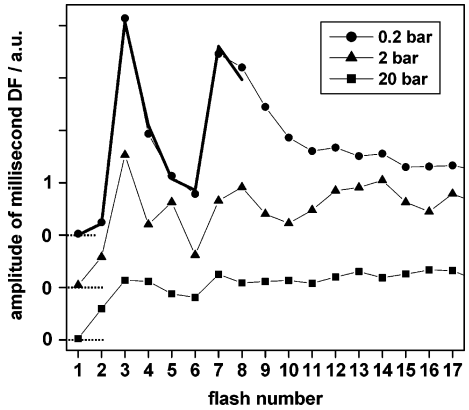

FIGURE 2: Flash patterns of the DF intensities integrated from 0.5 to 5 ms, at 0.2, 2.0, and 20 bar O_2. The integrated intensities after flash 1 were set to 0. The thick line was calculated with a miss factor of 7%, an initial population of 20% S_0 and 80% S_1, and a small exponentially rising offset (not shown) possibly because of the reduction of the quinone pool as function of the flash number.

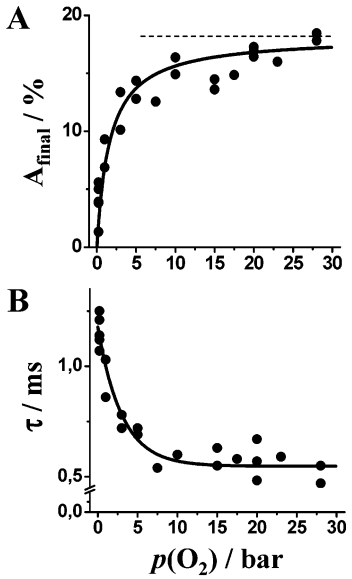

FIGURE 3: (A) Fraction of *A* ($S_3Y_Z^{ox}$) remaining in equilibrium after electron transfer in the O_2-evolving transition calculated according to $A_{final} = I_3/(I_2 + I_3)$. DF amplitudes ($I_i$) were obtained by triexponential simulations (see Table 1). The sum ($I_2 + I_3$) corresponds to the initial DF amplitude in the presence of $S_3Y_Z^{ox}$. I_2 denotes the magnitude of the millisecond DF kinetic component; I_3 is the level reached after $S_3Y_Z^{ox}$ reduction, i.e., essentially after S_0 formation at 0.2 bar O_2 and after S_2* formation at 20 bar O_2. The smooth line represents a fit according to eq 2, with parameters given in the Discussion. The dashed line denotes the equilibrium fraction of *A* at infinite $p(O_2)$. (B) Apparent time constant, τ, of the increase of *A*. The line represents an exponential simulation with $p(O_2)_{1/2} = 2.3$ bar.

$p(O_2)$ affected, however, slower DF phases, decaying in the time range between 0.5 and 5 ms (Figure 1C). The amplitude of these DF phases was diminished to about 35%. The decay time was accelerated from $\tau_2 \approx 1.2$ ms at ambient pressure to ~0.55 ms at 20 bar O_2 (Table 1). The DF transients on flash 4 and on higher flash numbers at 20 bar O_2 were very similar to that on flash 3 (data not shown). DF transients measured at 20 bar He (not shown) were essentially identical to those at 0.2 bar O_2, confirming that hydrostatic pressure per se does not affect the Mn → Y_Z^{ox} electron transfer, as previously observed (*6*). At 20 bar O_2, also on the 2nd flash, a minor portion of the DF decayed with a similar τ_2 of about 0.55 ms (Table 1) as observed on flash 3 (see also the next section).

The integrated DF amplitudes measured between 0.5 and 5 ms after each flash of a series and at three values of $p(O_2)$ are plotted in Figure 2. The pronounced period-of-four oscillation observed at 0.2 bar is well-described by a "miss" factor of 7% and assuming an initial population of 20% S_0 and 80% S_1 (Figure 2). Such parameters are frequently observed in flash experiments using highly active PSII membrane particles (*13*). After the 10th flash, the oscillations ceased because of complete reduction of the 5 plastoquinone molecules/PSII (*14*).

Already at 2 bar O_2, the extent of the DF in the millisecond time range was half-diminished, although still oscillatory (Figure 2). There were further differences of the flash pattern. The millisecond decay component was not only observed on flash 3 but also on flashes 2 and 5. Possibly, a fraction of centers underwent the O_2-evolving transition on these flashes (see the Discussion). Also noteworthy, at 2 bar O_2, oscillations were still detectable at flash numbers exceeding 10. This we attribute to the incomplete turnover of centers at lower flash numbers, suggesting that, on the average, less than one electron was stably transferred to the quinones.

At 20 bar O_2, the period-of-four oscillation was absent (Figure 2). Still, a small essentially nonoscillating DF amplitude in the 0.5−5 ms time range was detectable from the 3rd flash onward, suggesting relatively slow reduction of Y_Z^{ox} (slower than in the S_2 → S_3 transition induced by the 2nd flash). Its rate was similar on the 3rd and all later flashes (not documented), suggesting that the same reactions are induced by these flashes. The comparatively high DF amplitude at 10 ms observed from the 3rd flash onward indicates increased recombination losses. Therefore, we suggest that the state formed in the millisecond time range after the 3rd and later laser flashes at 20 bar O_2 decayed by recombination toward the S_3 state in the 700 ms interval between flashes so that from the 3rd flash onward each flash initiated the same sequence of events (and thus the same DF decay).

The DF decay was simulated by a sum of three exponentials (see Table 1) for DF transients induced by the 3rd flash and measured at $p(O_2)$ values ranging from 0.2 to 28 bar. The simulation results facilitated calculation of the equilibrium fraction of the initial state *A* (here assumed to be $S_3Y_Z^{ox}$) formed after the 3rd flash (Figure 3A, A_{final} calculated as detailed in the caption, see also the Discussion). A_{final} was <5% at 0.2 bar O_2 but increased to close to 20% at saturating $p(O_2)$. Concomitantly, the apparent relaxation time τ_2 (see Table 1) of the decay of *A* decreased from ~1.2 to ~0.55 ms (Figure 3B) (A slower DF relaxation time τ_3 of ~4.5 ms was present on all flashes. This phase mostly reflects reoxidation of Q_A^-, which was found to be relatively slow in the used PSII membrane particles (*15*) and appears to be pressure-independent). A more complex simulation approach of the DF transients on flash 3, e.g., using four exponentials, yielded a less pronounced decrease of τ_2 and a higher equilibrium fraction A_{final}. Employing a constant relaxation time τ_2 of 1.2 ms in the simulations yielded a maximum of A_{final} close to 40% (not documented).

DISCUSSION

UV spectroscopy on isolated PSII core particles from cyanobacteria subjected to elevated oxygen pressure has

provided evidence for at least one intermediate in the O_2-forming transition that tentatively has been ascribed to $(H_2O_2)S_2{*}Y_Z$, the 2-fold oxidized metal cluster with a bound peroxide (*6*). In this study, we applied an alternative method, delayed chlorophyll fluorescence, to corroborate and extend the above finding. Delayed fluorescence is distinguished by its high signal-to-noise ratio and applicability also to native PSII membranes (*7*). We find the pressure-dependent changes in the 3rd-flash DF transients of PSII membrane particles from plant material (spinach) to be compatible with the presence of an intermediate in the oxygen-evolving step, and we have used the same consecutive reaction scheme as in ref *6* for their interpretation. The common result of both approaches, UV spectroscopy and DF, is 50% inhibition of oxygen evolution already at a moderate $p(O_2)$ of 2.3 bar.

On the Origin of the Millisecond Phase on Flashes 2 and 5 at Elevated p(O₂). The observation of a DF phase with a millisecond decay time on the 2nd and 5th flash at elevated $p(O_2)$ is explainable by assuming that a $S_2{*}$ state is formed that converts to the normal S_2 state. One option for the $S_2{*} \rightarrow S_2$ conversion is the release of a peroxide bound to the metal complex in $S_2{*}$. This S_2 formation may occur via two alternative pathways. (i) Centers initially in the S_0 state are converted via $S_2{*} \rightarrow S_2$ in the dark. Assuming that about 20% of PSII is in S_0 in dark-adapted samples, the millisecond phase on the 2nd flash can be explained by this pathway. (ii) Centers present in state $S_2{*}$ after the 3rd flash are converted to S_2 in the time interval of 700 ms between flashes 3 and 4. The millisecond phase on the 5th flash may be explainable by either pathway. We feel that the present DF results represent a first indication that O_2 exerts a true backpressure also on the fully relaxed S_0 state, driving it backward via $S_2{*}$ to yield S_2. Proving the suggested $S_2{*}$ formation and peroxide release remains an important challenge for future research.

Energetics of the Final Transition during Water Oxidation. The DF component with $\tau_2 \approx 1.2$ ms at ambient $p(O_2)$ reflects the decay of the initial state in the below reaction scheme (denoted as *A*). It is assigned to the $S_3Y_Z^{ox}$ state, which decays in the O_2-forming transition in parallel to manganese reduction. At high $p(O_2)$, we find this decay to be accelerated ($\tau \approx 0.55$ ms), in line with the acceleration of the millisecond phase in the UV experiments (*6*, *11*, *12*). As in ref *6*, the following two-step reaction scheme is employed:

$$A \underset{b}{\overset{a}{\rightleftharpoons}} B \underset{d}{\overset{c}{\rightleftharpoons}} S_0Y_Z + O_2 \qquad (1)$$

where the intermediate state, *B*, is tentatively identified with $S_2{*}Y_Z$, a 2-fold reduced state of the catalytic metal center and *a*, *b*, *c*, and *d* are the rate constants of the respective forward and reverse reactions. The $p(O_2)$ dependence of A_{final}, the fraction of *A* remaining in equilibrium, then is given by

$$A(p(O_2))_{final} = \left[1 + \frac{a}{b}\cdot\left(1 + \frac{c}{d\cdot p(O_2)}\right)\right]^{-1} \qquad (2)$$

Simulation of the data points in Figure 3A based on eq 2 yielded ratios of $a/b = 5.0$ and $c/d = 1.2$ bar (—). Accordingly, with $\Delta G^{\circ\prime} = -k_BT \ln K$ ($k_B = 0.086$ meV K^{-1}, $T = 293$ K), a free-energy change of $\Delta G^{\circ\prime}(A \rightarrow S_2{*}Y_Z) = -40$ meV (for $K = a/b$) is calculated. This value represents the lower limit; an upper limit of -10 meV is obtained for an invariable time constant of 1.2 ms in the DF simulations. The respective value of $+17$ meV reported in ref *6* may be the upper limit; incorporation of the miss factor in the UV data analysis may render ΔG° negative. In summary, $S_2{*}$ formation is likely a downhill process, so that this state can accumulate to significant amounts.

For $\Delta G^{\circ\prime}(S_2{*}Y_Z \rightarrow S_0Y_Z + O_2)$, values of $-45/+71$ meV at 0.2/20 bar O_2 are calculated [for $K = c/dp(O_2)$]; the magnitude of $\Delta\Delta G^{\circ\prime}$ (the ΔG difference for 20 bar − 0.2 bar) of ≥ 100 mV is only weakly affected by the used simulation approach. In line with the conclusions reached in ref *6*, oxygen evolution at 20 bar O_2 is an energetically unfavorable uphill process, meaning that it practically does not proceed any more.

The above estimates by DF for the Gibbs free-energy profile of the reaction sequence (see eq 1) in part deviate from previous figures based on UV data (ref *6*). The differences may or may not result from a limited signal-to-noise ratio (in particular in the UV measurements) or from different material used in the UV (cyanobacterial PSII−core complexes) and in the DF studies (plant PSII membranes). More important than these differences is the common result, namely, the pronounced lowering of the driving force for the oxygen-evolving reaction by "O_2 backpressure" as evident from half-inhibition at only 10-fold higher oxygen pressure than ambient.

In conclusion, by exerting an oxygen backpressure affecting specifically the O_2-evolving step, we have a tool at hand to stabilize an intermediate of the water-splitting reaction for further spectroscopic analysis. Recent time-resolved X-ray absorption experiments provide evidence for another short-lived intermediate of the Mn complex, which is observable even at ambient oxygen pressure (*8*). The step-by-step dissection of the "inner sanctum" of PSII, the O_2-producing reaction, for its in-depth mechanistic understanding now may be within reach.

ACKNOWLEDGMENT

We thank M. Grabolle and J. Wichmann for valuable advice in the DF experiments and M. Fünning for excellent technical assistance in the preparation of the PSII membranes.

REFERENCES

1. Ferreira, K. N., Iverson, T. M., Maghlaoui, K., Barber, J., and Iwata, S. (2004) Architecture of the photosynthetic oxygen-evolving center, *Science 303*, 1831−1838.
2. Biesiadka, J., Loll, B., Kern, J., Irrgang, K.−D., and Zouni, A. (2004) Crystal structure of cyanobacterial photosystem II at 3.2 Å resolution: A closer look at the Mn-cluster, *Phys. Chem. Chem. Phys. 6*, 4733−4736.
3. Cinco, R. M., McFarlane, H. K. L., Robblee, J. H., Yano, J., Pizarro, S. A., Bellacchio, E., Sauer, K., and Yachandra, V. K. (2002) Calcium EXAFS establishes the Mn−Ca cluster in the oxygen-evolving complex of photosystem II, *Biochemistry 41*, 12928−12933.
4. Haumann, M., Müller, C., Liebisch, P., Iuzzolino, L., Dittmer, J., Grabolle, M., Neisius, T., Meyer-Klaucke, W., and Dau, H. (2005) Structural and oxidation state changes of the photosystem II manganese complex in four transitions of the water oxidation cycle ($S_0 \rightarrow S_1$, $S_1 \rightarrow S_2$, $S_2 \rightarrow S_3$, $S_{3,4} \Rightarrow S_0$) characterized by X-ray absorption spectroscopy at 20 K as well as at room temperature, *Biochemistry 44*, 1894−1908.
5. Kok, B., Forbush, B., and McGloin, M. (1970) Cooperation of charges in photosynthetic O_2 evolution-I. A linear four step mechanism, *Photochem. Photobiol. 11*, 457−475.

6. Clausen, J., and Junge, W. (2004) Detection of an intermediate of photosynthetic water oxidation, *Nature 430*, 480−483.
7. Grabolle, M., and Dau, H. (2005) Energetics of primary and secondary electron transfer in photosystem II membrane particles of spinach revisited on basis of recombination-fluorescence measurements, *Biochim. Biophys. Acta 1708*, 209−218.
8. Haumann, M., Liebisch, P., Müller, C., Barra, M., Grabolle, M., and Dau, H. (2005) Photosynthetic O_2 formation tracked by time-resolved X-ray experiments, manuscript in preparation.
9. Schiller, H., and Dau, H. (2000) Preparation protocols for high-activity photosystem II membrane particles of green algae and higher plants, pH dependence of oxygen evolution and comparison of the S_2-state multiline signal by X-band EPR spectroscopy, *J. Photochem. Photobiol. B 55*, 138−144.
10. Jeans, C., Schilstra, M. J., and Klug, D. R. (2002) The temperature dependence of P_{680}^+ reduction in oxygen-evolving photosystem II, *Biochemistry 41*, 5015−5023.
11. Clausen, J., and Junge, W. (2005) Search for intermediates of photosynthetic water oxidation, *Photosynth. Res. 84*, 339−345.
12. Clausen, J. (2004) Photosynthesische Wasseroxidation: Über Liganden und Zwischenprodukte, Doctoral Thesis, Universiät Osnabrück, Germany, http://elib.uni-osnabrueck.de.
13. Messinger, J., Schröder, W. P., and Renger, G. (1993) Structure−function relations in photosystem II. Effects of temperature and chaotropic agents on the period four oscillation of flash-induced oxygen evolution, *Biochemistry 32*, 7658−7668.
14. Kurreck, J., Seeliger, A. G., Reifarth, F., Karge, M., and Renger, G. (1995) Reconstitution of the endogenous plastoquinone pool in photosystem II (PS II) membrane fragments, inside-out-vesicles, and PS II core complexes from spinach, *Biochemistry 34*, 15721−15731.
15. Grabolle, M. (2005) Die Donorseite des Photosystems II der Pflanzen: Rekombinationsfluoreszenz und Röntgenabsorptionsstudien, Doctoral Thesis, Freie Universität Berlin, FB Physik, Germany.

BI051183A